

See discussions, stats, and author profiles for this publication at: <https://www.researchgate.net/publication/230710741>

Fovea Window for Wavelet-Based Compression

Conference Paper in Lecture Notes in Electrical Engineering · January 2011

DOI: 10.1007/978-1-4614-3535-8_55

CITATIONS

0

READS

54

4 authors, including:



J. C. Galan-Hernandez

Universidad de las Americas Puebla

8 PUBLICATIONS 22 CITATIONS

[SEE PROFILE](#)



Vicente Alarcon-Aquino

Universidad de las Americas Puebla

112 PUBLICATIONS 608 CITATIONS

[SEE PROFILE](#)



Oleg Starostenko

Universidad de las Americas Puebla

97 PUBLICATIONS 387 CITATIONS

[SEE PROFILE](#)

Some of the authors of this publication are also working on these related projects:



Fault detection and control of Induction motors and PMSM [View project](#)



Journal of Universal Computer Science, Special Issue "Advances in Security and Privacy of Multimodal Interfaces" [View project](#)

Chapter 55

Fovea Window for Wavelet-Based Compression

J. C. Galan-Hernandez, V. Alarcon-Aquino, O. Starostenko
and J. M. Ramirez-Cortes

Abstract Wavelet foveated compression can be used in real-time video processing frameworks for reducing the communication overhead while keeping high visual quality. Such algorithm leads into high rate compression results due to the fact that the information loss is isolated outside a region of interest (ROI). The fovea compression can also be applied to other classic transforms such as the commonly used the discrete cosine transform (DCT). In this paper, a fovea window for wavelet-based compression is proposed. The proposed window allows isolate a fovea region over an image. A comparative analysis has been performed showing different error and compression rates between the proposed fovea window for wavelet-based and the DCT-based compression algorithms. Simulation results show that with foveated compression high ratio of compression can be achieved while keeping high quality over the designed ROI.

J. C. Galan-Hernandez · V. Alarcon-Aquino · O. Starostenko
Department of Computing, Electronics and Mechatronics, Universidad de las Americas
Puebla, Sta. Catarina Martir, Cholula, 72810 Puebla. C.P., Mexico
e-mail: juan.galanhz@udlap.mx

V. Alarcon-Aquino
e-mail: vicente.alarcon@udlap.mx

J. M. Ramirez-Cortes (✉)
Department of Electronics, Instituto Nacional de Astrofisica, Optica y Electronica,
Tonantzintla, Puebla, Mexico
e-mail: olsovsky@fiit.stuba.sk

55.1 Introduction

Video processing is an intensive task and even more when it is restricted into a time window such as in real-time frameworks [1]. Compression algorithms can help to reduce communication overhead between computing nodes by reducing the redundancy of the data transmitted. Wavelet-based video compression algorithms achieve high ratios of compression. However, such algorithms also cause loss of information on video frames. In applications where a region of interest (ROI) can be isolated, foveation can be used in order to constraint the information loss only on those areas outside of the ROI in order to increase the quality of the reconstructed image. Several applications where ROIs over video frames can be identified can benefit from fovea compression such as medical video processing framework searching for melanomas by perform a lossy compression over the video frames, leaving the ROI intact for later processing. previous works in [2–4] show different foveation methods assessing the final quality of the image against the original image using human vision system (HVS) criteria. Foveation also guarantee certain quality from the HVS perspective granting the output results with enough quality for a user to inspect the ROI without noticing the loss of quality unless a close inspection outside the ROI is performed. In the work reported in this paper, a comparative analysis between wavelet-based and the DCT-based foveated compression algorithms is carried out. The remainder of this paper is organized as follows. In Sect. 55.2 an overview of foveated compression is given. Section 55.3 describes the proposed approach. Section 55.4 presents simulation results, and Sect. 55.5 presents conclusions and future work.

55.2 Foveated Compression

Wavelet transforms involve representing a general function in terms of simple, fixed building blocks at different scales and positions. These building blocks are generated from a single fixed function called mother wavelet by translation and dilation operations [5].

55.2.1 Wavelets and the Discrete Wavelet Transform

The purpose of wavelet transforms is to represent a signal into the time–frequency domain. To perform this task two functions are required, namely, a wavelet and a scaling function. If a set of mother wavelets and scaling functions is orthonormal it is called an orthonormal bases and is defined as follows [6]:

$$\{ \varphi_{l_0,n} \}_{0 \leq n \leq 2^{l_0}} \cup \{ \psi_{j,n} \}_{j < l_0, 0 \leq n \leq 2^j} \quad (55.1)$$

where 2^{l_0} is the size of the signal. Each $\psi_{j,n}$ is a translated copy of ψ at scale j :

$$\psi_{j,n}(t) = \sqrt{2^{-j}}\psi(2^{-j}t - n) \quad (55.2)$$

and each $\varphi_{l_0,n}$ is a translated copy of the scaling function φ at scale l_0 :

$$\varphi_{l_0,n}(t) = \sqrt{2^{-j}}\varphi(2^{-j}t - n) \quad (55.3)$$

For images, a two dimension wavelet transform is needed. In two dimensions, the decomposition ladder is constructed using three mother wavelets, $\psi_{j,m,n}^d$, $\psi_{j,m,n}^v$ and $\psi_{j,m,n}^h$ defined as follows [6]:

$$\psi_{j,m,n}^d = \psi_{j,m}(x)\psi_{j,n}(y) \quad (55.4)$$

$$\psi_{j,m,n}^v = \psi_{j,m}(x)\varphi_{j,n}(y) \quad (55.5)$$

$$\psi_{j,m,n}^h = \varphi_{j,m}(x)\psi_{j,n}(y) \quad (55.6)$$

with the scaling function:

$$\Phi_{j,m,n} = \varphi_{j,m}(x)\varphi_{j,n}(y) \quad (55.7)$$

where $\psi_{j,m,n}^d$ are the diagonal coefficients, $\psi_{j,m,n}^v$ are the vertical coefficients and $\psi_{j,m,n}^h$ are the horizontal coefficients. With the wavelet base defined, the next step is using it to represent a signal. The sum over all time of the signal multiplied by scaled, shifted versions of the mother wavelet ψ is given by

$$a_j(n) = \int_{-\infty}^{\infty} f(j)\psi(n,j)dt \quad (55.8)$$

where f is the signal to be represented. However, for compression this transform is not suitable because it expands the signal into more coefficients than the samples of the signal itself. A better transform, suited for compression and many other applications, is called the discrete wavelet transform (DWT). In [7], the DWT is calculated through a simple algorithm that applies two filters, a low pass filter and a high pass filter. This algorithm is known as the fast wavelet transform. In wavelet analysis of a signal f , we often speak of approximations and details. The approximations are the low-frequency components of the signal, see (55.9); whereas the details are the high-frequency components of the signal, see (55.10).

$$a_j[n] = \langle f, \varphi_{j,n} \rangle \quad (55.9)$$

$$d_j[n] = \langle f, \psi_{j,n} \rangle \quad (55.10)$$

55.2.2 Discrete Cosine Transform

The discrete cosine transform (DCT) expresses a signal in terms of cosine functions. Such transform is commonly used in the JPEG compression algorithm [8], the MP3 audio format and the VP8 video format. The discrete cosine transform for a signal $f(x)$ of length N is defined as follows [9]:

$$C(u) = \alpha(u) \sum_{x=0}^{N-1} f(x) \cos\left(\frac{\pi(2x+1)u}{2N}\right) \quad (55.11)$$

where $\alpha(u)$ is given by

$$\alpha(u) = \begin{cases} \sqrt{\frac{1}{N}} & \text{for } u = 0 \\ \sqrt{\frac{2}{N}} & \text{for } u \neq 0 \end{cases} \quad (55.12)$$

In particular, $C(u=0) = \sqrt{\frac{1}{N}} \sum_{x=0}^{N-1} f(x)$ is known as the direct current coefficient (DC) and the remaining coefficients are called the alternating current coefficients [10]. Most of the energy of the signal is packed in the DC coefficient.

55.2.3 Wavelet Compression

The objective of data compression is to represent a set of data with less information than the original. There are two types of compression, namely, lossy and lossless compression [10]. In lossy, some of the original data is discarded in order to achieve its goal. When the data is reconstructed it will be slightly different from the original. Lossy compression can help to achieve a better compression ratio than lossless compression if the losses are acceptable over the result. This is the standard practice on image compression such as in JPEG and in JPEG2000 formats [7, 10], and video such as MPEG4 format. When a wavelet transform is applied on an image, the resultant coefficients can then be compressed more easily because the information is statistically concentrated in just a few coefficients. Wavelet compression can reach higher compression ratio than other transforms such as the discrete cosine transform suggested for foveated compression in [3]. In wavelet lossy compression, the coefficients that contain the most amount of energy are preserved and the rest are discarded. Selecting such coefficients can be done using the wavelet energy profile and choosing a cutoff frequency.

55.2.4 Foveation

Foveated images are images which have a non-uniform resolution [6]. Results reported in [11] have demonstrated that the human eye shows a form of aliasing from

the fixation point to the edges of the image. Such aliasing increases in a logarithmic rate on all directions. This can be seen as concentric cutoff frequencies from the fixation point. When it is used in a wavelet, this can be expressed as a function [2]:

$$I_0(x) = \int I(t)C^{-1}(x)s\left(\frac{t-x}{w(x)}\right) \tag{55.13}$$

where $I(t)$ is a given image, $I_0(t)$ is the foveated image, $w(x)$ is the weight function. The function s is called the weighted translation of s by x . The function C is defined as:

$$C(x) = \left\| s\left(\frac{-x}{w(x)}\right) \right\| \tag{55.14}$$

There are several weighted translation functions such as the ones defined in [6]. In [3], the suggested weighted functions are the Hamming window (Fig. 55.1a) and the triangular (Fig. 55.1b) window. Such windows offer a smooth degradation from the fixation point. The results on a foveated image from [6] are shown in Fig. 55.2. However, in order to preserve a ROI intact, such windows are not useful. A ROI needs to be left with all its coefficients without cutoff. For well-defined ROIs windows such as Tukey window (Fig. 55.1c) or a truncated triangular window (Fig. 55.1d) can be used [12]. Such windows can be used to define a weighted function where the radio of a fixation point is bigger than one, leaving the coefficients from the ROI untouched and right after the ROI ends the energy begins to decay in a smooth ratio.

55.3 Proposed Fovea Method

55.3.1 Fovea Window

Fovea compression is expressed through a cutoff window. Ideal cutoff window is a logarithmic function as reported in [13]. Each pixel has a compression rate that decays radially respects to the fovea center. However, such function preserves only the center pixel of the fovea region. In order to create a fovea compression with a defined ROI bigger than one pixel, a fovea window function w is proposed as follows:

$$w(n) = \begin{cases} \ln(n * (e - 1) + 1) & \text{if } a \leq n \leq N \\ 1 & \text{if } n > N \end{cases} \tag{55.15}$$

where N is the radius in pixels of the fovea area, e denotes the Euler number, a is the radius also in pixels of the ROI and $n \in \mathbb{Z}^+$. Given a fovea center $F = (F_x, F_y)$ and a compression ratio interval $[b, L]$, the individual compression ratio $C_b^L(X, Y)$ of a pixel with coordinates $P = (X, Y)$ is calculated as follows:

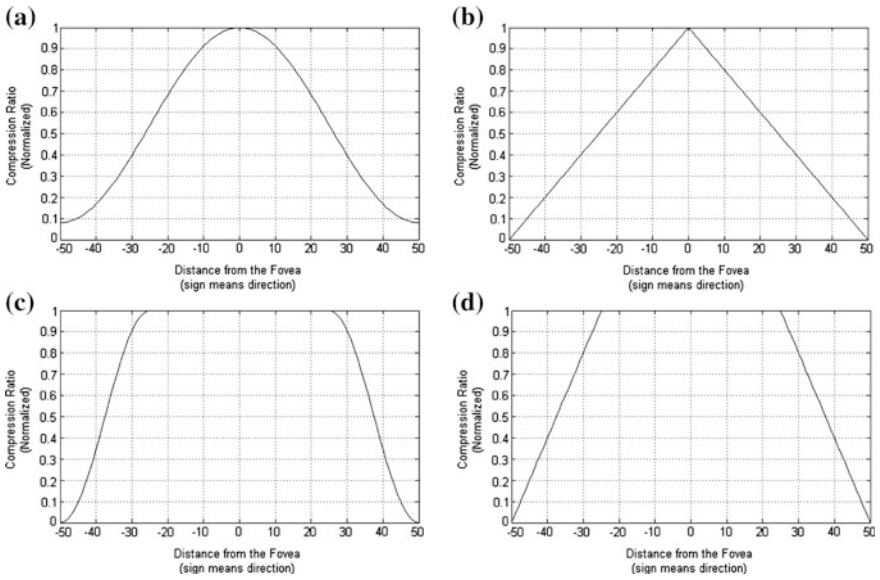


Fig. 55.1 Foveating windows. **a** Hamming window, **b** triangular window, **c** tukey window, **d** truncated triangular window



Fig. 55.2 An image and its wavelet foveated compression. **a** Original gray level image, **b** foveation point at the right eye

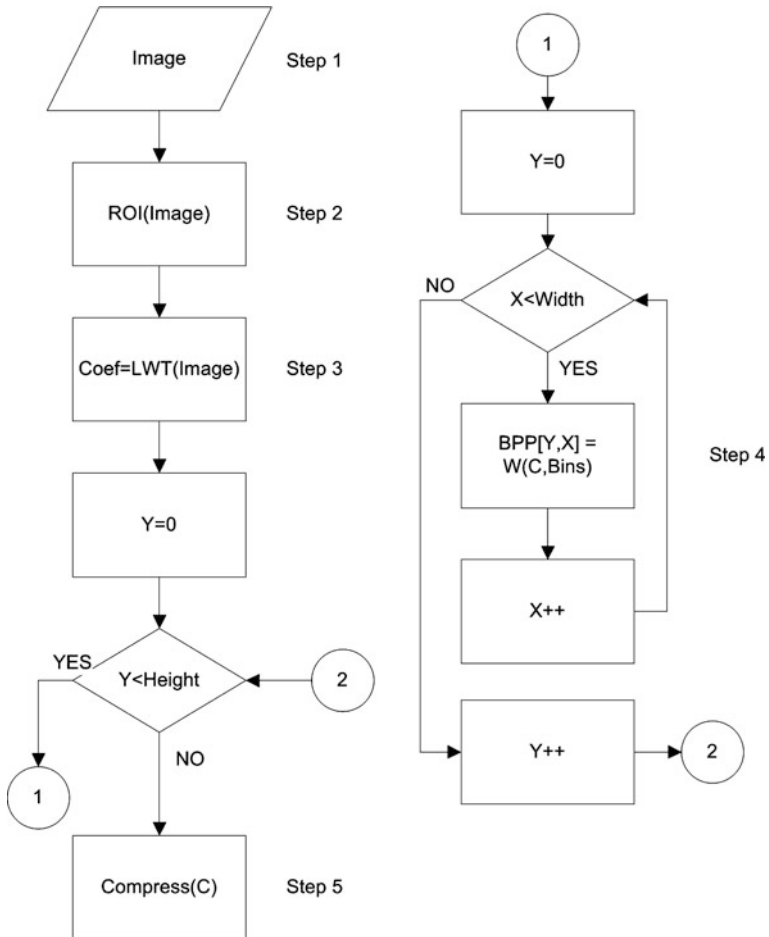


Fig. 55.3 Proposed Fovea compression Algorithm

$$C_b^L(P, F) = w \left(\frac{\|P - F\|}{N} \right) (L - b) + b \tag{55.16}$$

55.3.2 Proposed Algorithm

The proposed algorithm assumes that a method for calculating ROIs is given. The algorithm decomposes the image data into the frequency space using wavelets and the lifting wavelet transform (LWT) [14]. An image compressed through wavelets yields into a better visual quality when reconstructed than classic methods such as

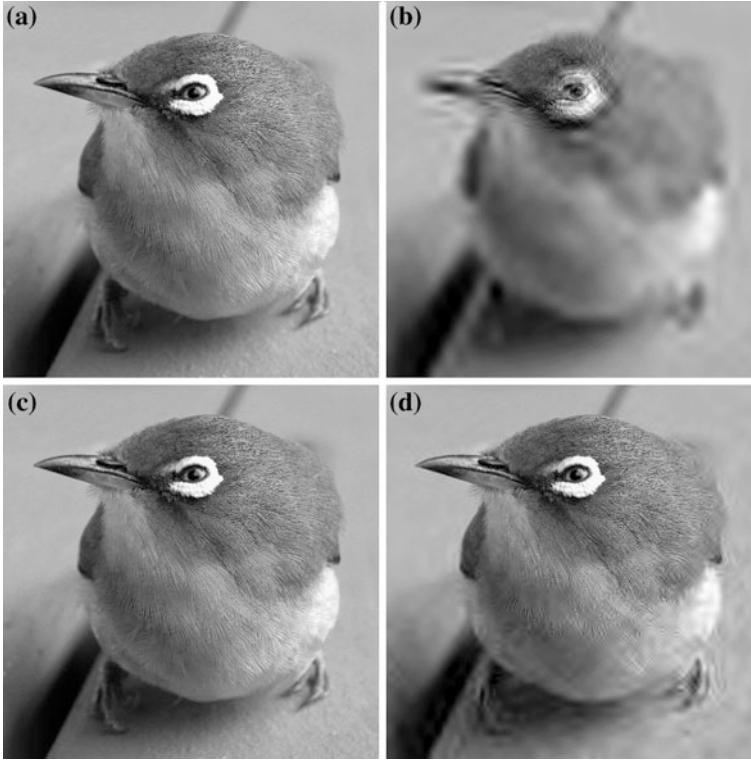


Fig. 55.4 Different foveating windows. **a** Original gray level image, **b** energy profile compression, **c** DCT-tukey window scaling quantization, **d** JPEG Type 1 quantization

the DCT [15]. The proposed algorithm is depicted in Fig. 55.3. The five main steps of the algorithm are:

1. *Image acquisition.*
2. *ROI calculation.*
3. *Wavelet coefficients calculation using the lifting wavelet transform (LWT).*
4. *The compression ratio of each coefficient is calculated.*
5. *A compression method is applied.*

The compression ratio, Eq. (55.16), is applied in step 4 to the wavelet coefficients. It is assumed that the relation of the wavelet coefficient with the pixel coordinates is given by a Quadtree with root at the 0-level of the wavelet decomposition. Given a coefficient of the wavelet located at an i -th level of the decomposition, the compression ratio in Eq. (55.16) can be rewritten as follows:

$$C_b^L(P, \frac{F}{2^i}) = w\left(\frac{2^i \|P - \frac{F}{2^i}\|}{N}\right)(L - b) + b \quad (55.17)$$

Table 55.1 Comparisons between wavelet-based foveated compression and DCT-based compression using the proposed window

| Wavelet | J | Zero coef. percentage | MSE | Quantization |
|---------|---|-----------------------|--------|-------------------|
| dct | – | 0.9383 | 2.2402 | JPEG-Type 3 |
| db7 | 2 | 0.3287 | 0.2534 | Tukey scaling |
| db7 | 4 | 0.3333 | 0.2503 | Tukey scaling |
| db9/7 | 2 | 0.3287 | 0.3279 | Tukey scaling |
| db9/7 | 4 | 0.3333 | 0.2428 | Tukey scaling |
| db7 | 2 | 0.8761 | 3.8959 | JPEG quantization |
| db7 | 4 | 0.9174 | 2.4795 | JPEG quantization |
| db9/7 | 2 | 0.8761 | 3.8167 | JPEG quantization |
| db9/7 | 4 | 0.9174 | 2.3974 | JPEG quantization |
| db7 | 2 | 0.9163 | 2.4192 | Energy profile |
| db7 | 4 | 0.9644 | 6.0816 | Energy profile |
| db9/7 | 2 | 0.9163 | 2.3897 | Energy profile |
| db9/7 | 4 | 0.9644 | 6.0116 | Energy profile |

where $P = (X, Y)$ are the coordinates of the coefficient on the matrix of the sub band of the wavelet decomposition at level i . Notice that each decomposition level has 3 sub bands and the last level of decomposition 4 sub bands [7]. In step 5, several compression methods can be used, namely, energy compression [16], JPEG quantization [17], and DCT-Tukey scaling [18]. Figure 55.4 shows an image and its reconstruction from different compression methods with the fovea point in the eye of the bird and a radius of 60 pixels, and four levels of wavelet decomposition using a Daubechies 7 wavelet.

55.4 Simulation Results

Simulations were carried out using the wavelets Daubechies 7 (db7) and Daubechies 9/7 (db9/7) suggested by the JPEG2000 standard [19] with two levels of decomposition, $J = 2$ for low image distortion using fovea compression and the JPEG200 standard level $J = 4$. To assess the performance of the wavelet-based foveated algorithm the mean squared error (MSE) metric is used. Also, an arbitrary fovea radius used was of 60 pixels. The results are shown in Table 55.1. The DCT-based foveated compression was also realized and it is shown in Table 55.1 as DCT. The compression was realized using the Type 3 JPEG variable quantization compression [8] and the proposed window in Eq. (55.16) as the quantization weight. Table 55.1 shows the percent of coefficients that becomes zero after the compression algorithm is applied to the original image. Figure 55.5 shows the DCT-based foveated image and a wavelet-based foveated image using the Daubechies 9/7 wavelet with four levels of decomposition with energy profile quantization, the proposed window-based scaling quantization and JPEG Type-1 quantization. It should be noted in Table 55.1 that the amount of zeros in the



Fig. 55.5 Foveated image with the proposed window and different compression methods. **a** DCT-based foveated compression, **b** wavelet-based foveated compression with db9/7 and energy profile quantization, **c** wavelet-based foveated compression with db9/7 and tukey window scaling quantization, **d** wavelet-based foveated compression with db9/7 and JPEG Type 1 quantization

coefficients after applying wavelet-based foveated algorithm using energy profile and JPEG Type-1 quantization schemes is lower than using the DCT-based approach. Furthermore, simulation results show that the DCT-based algorithm generates artifacts that make the image fuzzier than the wavelet-based algorithm.

55.5 Conclusion

Wavelet foveation compression offers a very good compression ratio at expenses of controlled losses. The proposed window allows isolate fovea regions over an image by choosing the slope. The fovea window has been applied over different algorithms showing the expected behavior. As stated in [3], applying foveation with wavelets yields into squared artifacts. These artifacts rise as the decomposition

levels increases. However, the DCT also showed a similar behavior in the area outside the ROI as the compression rate increases. With a good model for choosing a ROI, this kind of compression can achieve high compression ratios without losing visual quality over desired areas. Further work will focus on investigating other enhancements of the wavelet-based foveated compression algorithm and comparing with other methods such as the JPEG2000 ROI compression using the maximum shift (Maxshift) method [16].

Acknowledgments The authors gratefully acknowledge the financial support from the CONACYT Mexico and the Puebla State Government under the contract no. 109417.

References

1. N. Kehtarnavaz and M. Gamadia, “*Real-Time Image and Video Processing: From Research to Reality*,” Morgan and Claypool, University of Texas at Dallas, USA, 2006.
2. E. C. Chang and C. K. Yap, “A wavelet approach to foveating images,” In *SCG’97: Proceedings of the thirteenth annual symposium on Computational geometry*, New York, NY, USA, 1997, pp. 397–399.
3. S. Lee and A. Bovik, “Fast algorithms for foveated video processing,” *IEEE Transactions on Circuits and Systems for Video Technology*, Vol.13, No. 2, 2003, pp. 149–162.
4. Guo C, Zhang L (2010) A novel multiresolution spatiotemporal saliency detection model and Its applications in image and video compression. *IEEE Trans Image Process* 19(1):185–198
5. Boggess A, Narcowich FJ (2009) A first course in wavelets with Fourier analysis. 2nd edn. Wiley
6. E. C. Chang, S. Mallat, and C. Yap, “Wavelet Foveation,” in *Applied and Computational Harmonic Analysis*, Vol. 9, No. 3, 2000, pp. 312–335.
7. Mallat S (2008) A wavelet tour of signal processing. In: *The sparse way*, 3rd edn. Academic Press
8. Ahmad J, Raza K, Ebrahim M, Talha U (2009) FPGA based implementation of baseline JPEG decoder. In: *Proceedings of the 7th international conference on frontiers of information technology (FIT ’09)*. ACM, New York (Article 29)
9. N. Ahmed, T. Natarajan, and K. R. Rao, “Discrete cosine transform,” *IEEE Transactions on Computers*, Vol. C-32, January 1974, pp. 90–93.
10. Bovik AC (2009) *The essential guide to image processing*. Academic Press
11. B. A. Wandell. *Foundations of Vision*. Sinauer Associates, Inc., 1995.
12. Galan-Hernandez JC, Alarcon-Aquino V, Starostenko O, Ramirez-Cortes JM (2010) Wavelet-based foveated compression algorithm for real-time video processing. *IEEE Electron Robotics Automat Mech Conf (CERMA’10)* pp 405–410
13. Chang E (2000) Wavelet foveation. *Appl Comput Harm Anal* 9(3):312–335
14. C. Jain, V. Chaudhary, K. Jain, S. Karsoliya. “Performance analysis of integer wavelet transform for image compression,” *3rd International Conference on Electronics Computer Technology (ICECT’11)*, Vol.3, April 2011, pp.244–246.
15. I. Bocharova, “*Compression for Multimedia*,” 1st ed. Cambridge University Press, New York, NY, USA, 2010.
16. M. Mrak, M. Grgic, and M. Kunt, “*High-Quality Visual Experience*,” *Signals and Communication Technology Series*, Springer-Verlag, Berlin, 2010.
17. Richter T (2010) Spatial constant quantization in JPEG XR is nearly optimal. *Data compression conference (DCC’10)*, March 2010, pp79–88

18. J. C. Galan-Hernandez, V. Alarcon-Aquino, O. Starostenko, and J. M. Ramirez-Cortes, "Foveated ROI compression with hierarchical trees for real-time video transmission," *In Proceedings of the Third Mexican conference on Pattern recognition (MCPR'11)*, Springer-Verlag, Berlin, Heidelberg, 2011, pp. 240-249.
19. E. J. Balster, B. T. Fortener, W. F. Turri, "Integer Computation of Lossy JPEG2000 Compression," *IEEE Transactions on Image Processing*, Vol. 20, No.8, 2011, pp.2386-2391.